



Champneys, AR., Haerterich, J., & Sandstede, B. (1994). *A non-transverse homoclinic orbit to a saddle-node equilibrium*.
<http://hdl.handle.net/1983/313>

Early version, also known as pre-print

[Link to publication record in Explore Bristol Research](#)
PDF-document

University of Bristol - Explore Bristol Research

General rights

This document is made available in accordance with publisher policies. Please cite only the published version using the reference above. Full terms of use are available:
<http://www.bristol.ac.uk/red/research-policy/pure/user-guides/ebr-terms/>

A non-transverse homoclinic orbit to a saddle-node equilibrium.

Alan R. Champneys

Department of Engineering Mathematics

University of Bristol

Queen's Building, University Walk

Bristol BS8 1TR, UK

Jörg Härterich

Institut für Mathematik I

Freie Universität Berlin

Arnimallee 2-6

14195 Berlin, Germany

Björn Sandstede

Weierstraß-Institut für Angewandte Analysis und Stochastik

Mohrenstraße 39

10117 Berlin, Germany

Abstract

A homoclinic orbit is considered for which the center-stable and center-unstable manifolds of a saddle-node equilibrium have a quadratic tangency. This bifurcation is of codimension two and leads generically to the creation of a bifurcation curve defining two independent transverse homoclinic orbits to a saddle-node. This latter case was shown by L.P. Shilnikov to imply shift dynamics. It is proved here that in a large open parameter region of the codimension-two singularity, the dynamics are completely described by a perturbation of the Hénon-map giving strange attractors, Newhouse sinks and the creation of the shift dynamics. In addition, an example system admitting this bifurcation is constructed and numerical computations are performed on it.

1 Introduction

In recent years several authors have investigated the bifurcations in flows caused by codimension-two homoclinic orbits. See, for example, [Fie92], [San93], [CK94] and references therein. In this article we are interested in a homoclinic solution $q(t)$ converging to

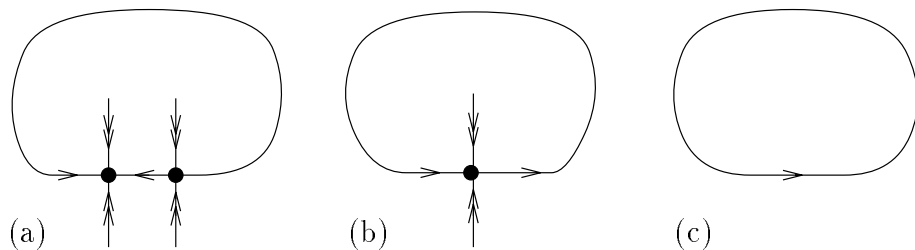


Figure 1: Planar bifurcation of a homoclinic solution to a saddle-node equilibrium

a non-hyperbolic equilibrium p_0 , which undergoes a saddle-node bifurcation. This situation is in fact of codimension one. Indeed, generically the homoclinic orbit is contained in the transverse intersection of the center-stable and center-unstable manifolds of the equilibrium p_0 . Therefore, the orbit $\gamma(q)$ together with the stationary point p_0 form a normally hyperbolic manifold diffeomorphic to S^1 , see figure 1(b).

Note that the normally hyperbolic manifold persists even under perturbations that break the saddle-node. It is easy to determine the flow on that manifold. Either two heteroclinic orbits appear connecting the two equilibria which bifurcate from the saddle-node p_0 or the manifold just consists of a periodic orbit, see figure 1(a),(c). Note that for systems in more than two dimensions, it is of no extra codimension for more than one homoclinic orbit to exist simultaneously to the same saddle-node. Moreover, if there are multiple - say k - such distinct homoclinic solutions, Shilnikov [Shi69] proved that the Poincaré map restricted to the invariant set in a neighborhood of the union of these homoclinic orbits is conjugate to a shift on k symbols under a parameter variation such that the stationary point disappears.

One of the objectives of this article is to show how a system may arise in which two homoclinic solutions to a saddle-node equilibrium are present. To that end, we investigate the following bifurcation of codimension two. We assume the existence of a saddle-node equilibrium with center-stable and center-unstable manifolds both of dimension at least two and such that their intersection fails to be transverse. Instead these manifolds should possess a quadratic tangency at an intersection point $q(0)$, see figure 2. This corresponds to a “saddle-node” bifurcation of two homoclinic solutions which collide and disappear as a parameter is varied. At the same time, the horseshoe proved to exist by Shilnikov [Shi69] has to be annihilated, too. We will show that this annihilation process is precisely

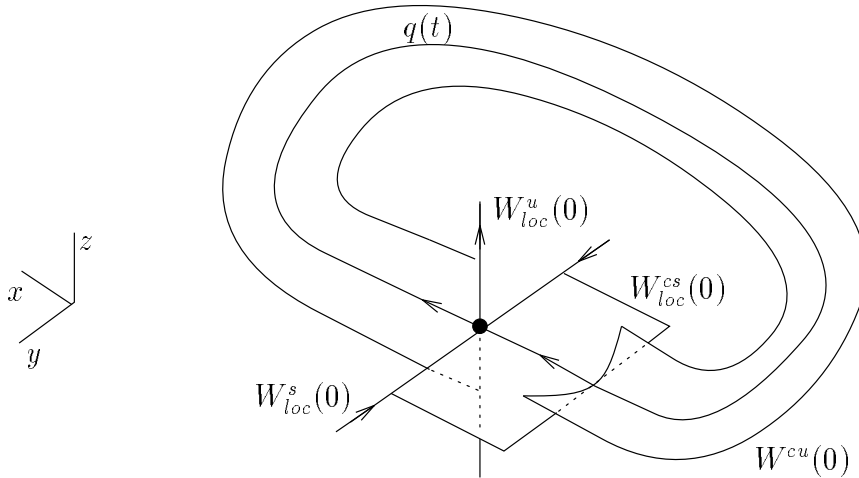


Figure 2: A degenerate homoclinic orbit to a saddle-node equilibrium

given by the dynamics of a Hénon-like map. In fact, the Poincaré map in a neighborhood of the homoclinic orbit turns out to be a small perturbation of the logistic map, under a suitable scaling. Therefore, all phenomena like persistent homoclinic tangencies of periodic orbits, infinitely many Newhouse sinks and period doubling sequences known to occur in the Hénon map [PT93] are proved to exist for the unfolding of the degenerate homoclinic orbit. We will discuss these issues as well as others in more detail in the last section.

Let us finally mention the related result on another bifurcation of codimension two involving a homoclinic orbit to a saddle-node. Here the homoclinic solution is contained in the intersection of, say, the center-unstable manifold with the stable manifold. The corresponding scenario has been extensively studied in the literature, see [Luk82, Sch87] for the two-dimensional case and [CL90, Den90] in higher dimensions. Essentially, this bifurcation occurs on a two-dimensional manifold due to a homoclinic center-manifold reduction, see [San93]. In contrast, we are unaware of any previous treatment of the case under investigation here other than a certain index-theory result in [Fie92], see the Discussion for more details.

The rest of this paper is organised as follows. In section 2 we state our main result and in section 3 we prove it. As with many results in homoclinic bifurcation theory, we shall state our theorem for systems of the lowest possible dimension only, in this case three dimensions.

However, using center-manifold results for homoclinic orbits as in [San93, San94a] it should be easily possible to show the results to hold for systems in \mathbb{R}^n for arbitrary $n \geq 3$. Then, in section 4, we present an equation which will be proved to admit a non-transversal homoclinic orbit to a saddle-node equilibrium as well as to possess a generic unfolding. Although an artificial example, it allows for illustration of the preceding theory and serves as a test example. Numerical methods are used to detect the codimension-two point and to demonstrate the asymptotic scalings. In the last section we give conclusions and discuss the relevance of our results to applications.

Acknowledgement. We thank Bernold Fiedler and Arnd Scheel for helpful discussions. Collaboration was made possible through the support of WIAS and the visiting fellow research grant GR/K/39653 from the U.K. EPSRC.

2 The main results

Consider the equation

$$(2.1) \quad \dot{u} = f(u, \mu), \quad (u, \mu) \in \mathbb{R}^3 \times \mathbb{R}^2.$$

We assume that f is sufficiently smooth and that 0 is an equilibrium of (2.1) for $\mu = 0$ such that

$$(H1) \quad \sigma(D_u f(0, 0)) = \{-\lambda^s, 0, \lambda^u\} \text{ and } \lambda^s \neq \lambda^u \text{ as well as } -\lambda^s < 0 < \lambda^u.$$

Furthermore, suppose that $q(t)$ is a homoclinic orbit converging to 0 as t tends to $\pm\infty$, which is neither contained in the stable nor the unstable manifold of 0 , i.e.

$$(H2) \quad q(0) \in W^{cs}(0) \cap W^{cu}(0) \quad \text{but} \quad q(0) \notin W^s(0) \cup W^u(0).$$

Here $W^{cs}(0)$ and $W^{cu}(0)$ denote respectively the center-stable and center-unstable manifolds of 0 , see e.g. [Van89]. Moreover, we assume that the intersection in hypothesis (H2) is not transverse, i.e.

$$(H3) \quad W^{cs}(0) \text{ and } W^{cu}(0) \text{ have a quadratic tangency at } q(0).$$

In the appendix an analytical expression involving the nonlinearity of f only is derived which determines whether the tangency is quadratic or of higher order. Now, we have to impose non-degeneracy conditions on the dependence of the nonlinearity on the parameters μ . The saddle-node equilibrium and the quadratic tangency must unfold generically but independently of each other. To this end, we define v_c and w_c to be respectively the right and left eigenvectors corresponding to the zero eigenvalue, the existence of which is ensured by hypothesis (H1). Moreover, let $\psi(t)$ be the unique bounded solution of the adjoint variational equation

$$\dot{w} = -D_u f(q(t), 0)^T w,$$

see [San93] for further properties of this equation. Note that

$$\psi(t) \in (T_q(t)W^{cs}(0) + T_q(t)W^{cu}(0))^\perp$$

exists and decays exponentially to zero for $t \rightarrow \pm\infty$ due to hypothesis (H3).

Define

$$(2.2) \quad \begin{aligned} M &= \int_{-\infty}^{\infty} \langle \psi(t), D_\mu f(q(t), 0) \rangle dt \\ N &= \langle w_c, D_\mu f(0, 0) \rangle, \end{aligned}$$

which are vectors in the parameter space \mathbb{R}^2 . In fact, M is the usual Melnikov integral measuring the rate of splitting of the center-stable and center-unstable manifolds. Then the non-degeneracy conditions are given as follows.

- (H4) (i) $\langle w_c, D_u^2 f(0, 0)[v_c, v_c] \rangle \neq 0$
(ii) M and N are linearly independent in \mathbb{R}^2 .

Hypothesis (H4)(i) is equivalent to the fact that the vector field restricted to the center

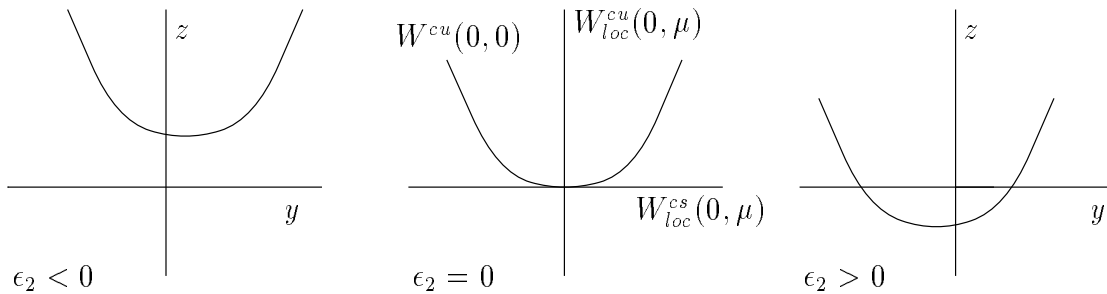


Figure 3: The unfolding of the quadratic tangency

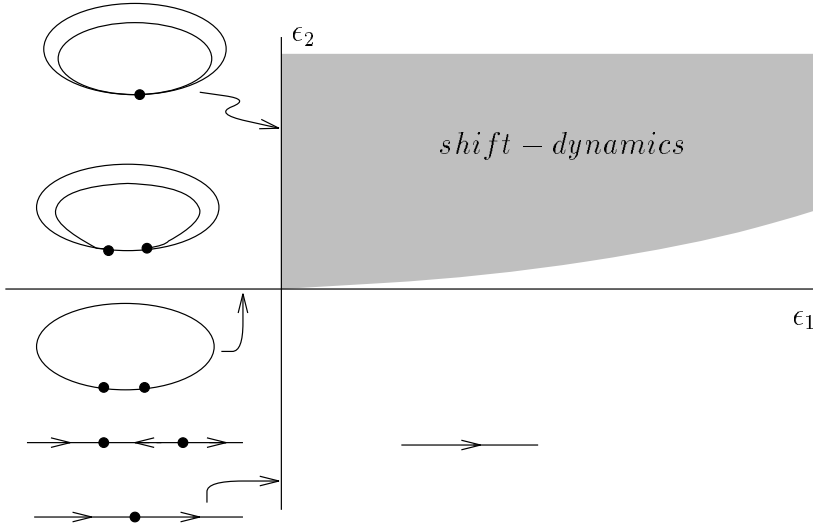


Figure 4: The bifurcation diagram

manifold possesses a non-zero quadratic term for $\mu = 0$. Owing to (H4)(ii) the saddle-node and the quadratic tangency of center-stable and center-unstable manifolds unfold generically and independently with respect to the two-dimensional parameter μ , see section 3.

Now we can state our main result.

Theorem 1 *Suppose that the assumptions (H1) up to (H4) are satisfied. Furthermore, assume $\lambda^u < \lambda^s$, otherwise reverse time. Then, after a change of parameters $\epsilon = \epsilon(\mu)$, we obtain the bifurcation diagram given in figure 4.*

Here the positive ϵ_1 -axis consists of saddle-nodes of periodic orbits. There exists no recurrent dynamics for $\epsilon_1 > 0$, $\epsilon_2 < 0$. Moreover, the Poincaré map defined on a transverse section is conjugate to a perturbed Hénon map

$$(y, z) \mapsto (z, z^2 + \delta) + \mathcal{O}(e^{\pm c/\sqrt{\epsilon_1}} (|y| + |z|, |z|^2 + |y|))$$

on each line $\epsilon_1 = \text{const.} > 0$. The error estimate is valid in the C^3 -topology. Here $\delta = e^{2C(\epsilon)\lambda^u/\sqrt{\epsilon_1}}\epsilon_2$ for some function $C(\epsilon)$ smooth for positive ϵ_1 such that $C(0) > 0$. Hence, changing $\epsilon_2 \in [-\eta, \eta]$ corresponds to varying $\delta \in [-\eta e^{c/\sqrt{\epsilon_1}}, \eta e^{c/\sqrt{\epsilon_1}}]$ for some fixed $c > 0$.

In particular, we have the following corollary.

Corollary 1 *The Poincaré map for $\epsilon_1 > 0$ contains period doubling sequences, persistent homoclinic tangencies to periodic points and infinitely many periodic sinks. Moreover, strange attractors exist.*

Proof. This follows from the results obtained by Yorke and Alligood [YA85], Mora and Viana [MV93], and Palis and Takens [PT93], to which the reader is also referred for more details of the bifurcation sequences giving rise to these diverse dynamical regions. \square

The function $C(\epsilon)$ appearing in the scaling of the parameter $\delta = e^{2C(\epsilon)\lambda^u/\sqrt{\epsilon_1}}\epsilon_2$ does essentially not depend on the eigenvalues λ^s and λ^u . Hence the scaling involves only the eigenvalue closest to zero which we have assumed to be λ^u .

3 The proof

Throughout, we assume that hypotheses (H1) to (H4) are satisfied. The geometry of the problem under investigation is depicted in Figure 2. First, we choose coordinates such that

$$\begin{aligned} W_{loc}^c(0, \mu) &= \{(x, 0, 0) \mid |x| < \eta\} \\ W_{loc}^{cs}(0, \mu) &= \{(x, y, 0) \mid |x| + |y| < \eta\} \\ W_{loc}^{cu}(0, \mu) &= \{(x, 0, z) \mid |x| + |z| < \eta\} \end{aligned}$$

for all μ satisfying $|\mu| < \eta$ for some small $\eta > 0$. We define

$$\Sigma_{\pm} := \{(\pm\Delta, y, z) \mid |y| + |z| < \eta\}$$

as sections transverse to the homoclinic solution. Then we can parametrize $W^{cu}(0, \mu) \cap \Sigma_{\perp}$ as a function over $W_{loc}^{cs}(0, \mu) \cap \Sigma_{\perp}$, i.e.

$$(3.1) \quad W^{cu}(0, \mu) \cap \Sigma_{\perp} = \{(-\Delta, y, z) \mid z = G(y, \mu) = (1 + G_1(y, \mu))y^2 + G_2(\mu)y + G_3(\mu)\},$$

see Figure 3. Here $G_i(0, 0) = 0$ for $i = 1, 2, 3$. Observe that the coefficient of the quadratic term can be chosen to be unity for $\mu = 0$ without loss of generality. Denote the unique minimum of $G(\cdot, \mu)$ near $(0, 0)$ by $Y(\mu)$. Then we define

$$\hat{G}(\mu) := G(Y(\mu), \mu).$$

The next lemma gives a connection between the vectors M and $D_{\mu}\hat{G}(0)$.

Lemma 1 *The relation $D_\mu \hat{G}(0) = c M$ holds for some $c \neq 0$.*

Proof. Note first that the constant c is due to the coordinate transformation at the beginning of this section, which did not involve a change of parameters. By the geometrical interpretation of the Melnikov integral as the rate of splitting of the center-stable and center-unstable manifolds, under parameter variation, it is clear that the vector M will not change its direction under this coordinate transformation. In the new coordinates we will actually show that

$$D_\mu \hat{G}(0) = M.$$

To verify this equality, compute

$$\hat{G}(\mu) = (1 + G_1(Y(\mu), \mu)) \left(\frac{G_2(\mu)}{2} \right)^2 - \frac{G_2(\mu)^2}{2} + G_3(\mu) + \mathcal{O}(\mu^2),$$

using (3.1). Then

$$D_\mu \hat{G}(0) = D_\mu G_3(0)$$

as the G_i vanish for $\mu = 0$. On the other hand, by construction, the splitting distance is given by the vertical component $\hat{G}(\mu)$. The Melnikov integral, defined as the derivative of the splitting distance at $\mu = 0$, is therefore given by

$$M = D_\mu G_3(0).$$

This proves the lemma. □

In the proof of Theorem 1 we will make use of a C^k -normal form near 0 which is given by Il'yashenko and Yakovenko in [IY91, Thm. 5]. They consider a parametrized family of vector fields near an equilibrium with the property that for the parameter value $\mu = 0$ there exists an equilibrium the linearization of which has a single zero eigenvalue. Then for arbitrarily large $k \in \mathbf{N}$ this family is locally C^k -conjugate to the vector fields induced by

$$\begin{aligned} \dot{x} &= \sum_{i=0}^{m+2} a_i(\mu) x^i + x^m + a(\mu) x^{2m+1} \\ \dot{y} &= -\alpha(x, \mu) y \\ \dot{z} &= \beta(x, \mu) z. \end{aligned}$$

Here $m \geq 2$ is the multiplicity of the zero of the vector field at $\mu = 0$, and α, β and the a_i are C^k -functions with $\alpha(0, 0) = \lambda^s$, $\beta(0, 0) = \lambda^u$ and $a(0) = a_i(0) = 0$ for all i . In our

case $m = 2$, since condition (H4)(i) implies that the vector field restricted to the center manifold has a double zero at 0 for $\mu = 0$, see [Sot74, GH90]. Furthermore, we will perform a change of parameters $\epsilon = \epsilon(\mu)$ such that $a_0(\mu) = \epsilon_1$. At the moment, ϵ_2 has yet to be defined. For definiteness, we will suppose that $D_{\epsilon_2} \hat{G}(0) < 0$ such that the center-stable and center-unstable manifold intersect each other for $\epsilon_2 \geq 0$, see Figure 3.

The normal form near $(0, 0)$ then reads

$$(3.2) \quad \begin{cases} \dot{x} &= \epsilon_1 + x^2(1 + a(\epsilon)x) \\ \dot{y} &= -\alpha(x, \epsilon)y \\ \dot{z} &= \beta(x, \epsilon)z. \end{cases}$$

The normal form transformation thus “almost” linearizes the vector field.

3.1 The case $\epsilon_1 \leq 0$

The normal form (3.2) already shows that for $\epsilon_1 \leq 0$ there will be no recurrence inside a tubular neighborhood of $q(\cdot)$. Note that in this case there are two equilibria $(x_1^*, 0, 0)$ and $(x_2^*, 0, 0)$ with invariant planes given by $x = x_1^*$ and $x = x_2^*$ between which the x -component of the vector field is negative, see figure 1(a).

To verify our statements about homoclinic and heteroclinic orbits, note that (3.1) and Lemma 1 describe exactly how the center-unstable manifold intersects the local center-stable manifold. Varying ϵ_2 basically shifts the parabola in figure 3 up and down. Thus, for $\epsilon_2 < 0$ there will be no intersection of the two manifolds. For $\epsilon_2 = 0$ there will be exactly one point of intersection corresponding to either a homoclinic orbit (if $\epsilon_1 = 0$) or to a heteroclinic connection between the two equilibria that arise from the saddle-node bifurcation (in the case $\epsilon_1 < 0$).

For $\epsilon_2 > 0$, there will be two points of intersection between the parabola $W^{cu}(0, \epsilon) \cap \Sigma_\perp$ and the y -axis in Σ_\perp , leading to two homoclinic respectively two heteroclinic orbits.

3.2 The case $\epsilon_1 > 0$

For this case we are going to show the conjugacy to a Hénon map as claimed in Theorem 1. This will be achieved via a sequence of lemmata. In the following, we assume without loss of generality that $\lambda^u < \lambda^s$ holds. Otherwise, we consider the vector field with time

reversed.

We begin with the calculation of the Poincaré map near the homoclinic orbit. Recall the definition of the two sections

$$\Sigma_{\pm} = \left\{ (\pm\Delta, y, z) \mid |y| + |z| < \eta \right\}.$$

Between those sections we will consider the flow-induced maps $\Pi_{loc} : \Sigma_{\perp} \rightarrow \Sigma_{+}$ and $\Pi_{far} : \Sigma_{+} \rightarrow \Sigma_{\perp}$.

The normal form (3.2) enables us to give a sufficiently accurate estimate for Π_{loc} while the assumption (H3) on the quadratic tangency between $W^{cs}(0)$ and $W^{cu}(0)$ is essential for estimating Π_{far} .

Lemma 2 *The local Poincaré map $\Pi_{loc} : \Sigma_{\perp} \rightarrow \Sigma_{+}$ is given by*

$$(3.3) \quad \Pi_{loc}(y, z) = \left(e^{\pm \frac{C(\epsilon)\lambda^s}{\sqrt{\epsilon_1}}} y, e^{\frac{C(\epsilon)\lambda^u}{\sqrt{\epsilon_1}}} z \right),$$

where $C(\epsilon)$ is a smooth function of ϵ and $\tilde{C}_1 \leq C(\epsilon) \leq \tilde{C}_2$ for some positive constants \tilde{C}_1 and \tilde{C}_2 . The mapping Π_{loc} is C^k with respect to ϵ_2 .

Proof. We start with a calculation of the “time of flight” between the sections Σ_{\perp} and Σ_{+} . The flow is induced by the normal form (3.2). We assume here that the sections are taken in such a way that, for all $|y|, |z| < \eta$ and $|x| \leq \Delta$, we have $|a(\epsilon)\Delta| < \frac{1}{2}$ and

$$0 < C_1 \leq \frac{\alpha(x, \epsilon)}{\alpha(0, 0)}, \quad \frac{\beta(x, \epsilon)}{\beta(0, 0)} \leq C_2$$

for some positive constants C_1 and C_2 . Note that the x -equation of (3.2) does not depend on y or z and hence can be integrated. This leads to

$$t(x) = \int_{\pm\Delta}^x \frac{1}{\epsilon_1 + w^2 + a(\epsilon)w^3} dw.$$

The equation

$$\dot{y} = -\alpha(x, \epsilon)y$$

thus implies

$$y(t) = y(0) \exp \left(- \int_0^t \alpha(x(\tau), \epsilon) d\tau \right).$$

Writing Π_{loc} in the form $(-\Delta, y_{in}, z_{in}) \mapsto (\Delta, y_{out}, z_{out})$, we arrive at

$$\begin{aligned}
y_{out} &= y_{in} \exp \left(- \int_0^{t(\Delta)} \alpha(x(\tau), \epsilon) d\tau \right) \\
(3.4) \quad &= y_{in} \exp \left(- \int_{\perp\Delta}^{\Delta} \frac{\alpha(x, \epsilon)}{\epsilon_1 + x^2 + a(\epsilon)x^3} dx \right).
\end{aligned}$$

Since the integral in the exponent does not depend on y or z , it can be estimated by

$$\int_{\perp\Delta}^{\Delta} \frac{C_1 \alpha(0, 0)}{\epsilon_1 + \frac{3}{2}x^2} dx \leq \int_{\perp\Delta}^{\Delta} \frac{\alpha(x, \epsilon)}{\epsilon_1 + x^2 + a(\epsilon)x^3} dx \leq \int_{\perp\Delta}^{\Delta} \frac{C_2 \alpha(0, 0)}{\epsilon_1 + \frac{1}{2}x^2} dx.$$

Calculating explicitly the integrals on the left and right hand sides we get

$$\frac{\tilde{C}_1 \alpha(0, 0)}{\sqrt{\epsilon_1}} \leq \int_{\perp\Delta}^{\Delta} \frac{\alpha(x, \epsilon)}{\epsilon_1 + x^2 + a(\epsilon)x^3} dx \leq \frac{\tilde{C}_2 \alpha(0, 0)}{\sqrt{\epsilon_1}}$$

for some positive constants \tilde{C}_1 and \tilde{C}_2 independent of y , z and ϵ . Therefore, there exists a C^k -function

$$C(\epsilon) := \frac{\sqrt{\epsilon_1}}{\alpha(0, 0)} \int_{\perp\Delta}^{\Delta} \frac{\alpha(x, \epsilon)}{\epsilon_1 + x^2 + a(\epsilon)x^3} dx$$

with $0 < \tilde{C}_1 \leq C(\epsilon) \leq \tilde{C}_2$ such that

$$y_{out} = y_{in} e^{\perp \frac{C(\epsilon) \alpha(0, 0)}{\sqrt{\epsilon_1}}} = y_{in} e^{\perp \frac{C(\epsilon) \lambda^s}{\sqrt{\epsilon_1}}}.$$

The same arguments apply also to the z -equation and in exactly the same manner we get

$$z_{out} = z_{in} e^{\frac{C(\epsilon) \beta(0, 0)}{\sqrt{\epsilon_1}}} = z_{in} e^{\frac{C(\epsilon) \lambda^u}{\sqrt{\epsilon_1}}}.$$

For later purposes we need to show that Π_{loc} is differentiable with respect to ϵ_2 . That this holds true is obvious from the integral representation (3.4) as the denominator never vanishes for $|y|, |z| < \eta$, $|x| \leq \Delta$. Inductively, it can be shown that y_{out} and z_{out} are k -times differentiable with respect to ϵ_2 . \square

Lemma 3 *After an appropriate coordinate transformation*

$$\begin{aligned}
(3.5) \quad y &= \tilde{y} + g(\epsilon) \\
z &= \tilde{z} + e^{\perp \beta} h(\epsilon) = \tilde{z} + e^{\perp \frac{C(\epsilon) \lambda^u}{\sqrt{\epsilon_1}}} h(\epsilon)
\end{aligned}$$

the Poincaré map $\Pi = \Pi_{far} \circ \Pi_{loc}$ takes the form

$$\Pi(y, z, \epsilon) = \begin{pmatrix} e^\beta z + b e^{\perp\alpha} y \\ e^{2\beta} z^2 + c e^\beta z + \epsilon_2 \end{pmatrix} + \mathcal{O} \begin{pmatrix} (e^{\perp\alpha} |y| + e^\beta |z|) (e^{\perp\alpha} |y| + e^\beta |z| + |\epsilon|) \\ (e^{\perp\alpha} |y| + e^{2\beta} |z|^2) (e^{\perp\alpha} |y| + e^\beta |z| + |\epsilon|) \end{pmatrix}$$

for some $b, c \in \mathbb{R}$. Here we have set as abbreviations $e^{\perp\alpha} := e^{\perp \frac{C(\epsilon)\lambda^s}{\sqrt{\epsilon^1}}}$ and $e^\beta := e^{\frac{C(\epsilon)\lambda^u}{\sqrt{\epsilon^1}}}$, while $\mathcal{O}(\cdot)$ denotes the Landau order symbol.

Proof. Owing to the quadratic tangency condition (H3) and by stretching the y - and z -axis appropriately, Π_{far} can be written in the general form

$$\begin{pmatrix} \Delta \\ y \\ z \end{pmatrix} \mapsto \begin{pmatrix} -\Delta \\ z + f_1(z, \epsilon) z + b_1 y + f_2(y, z, \epsilon) y + f_3(\epsilon) \\ z^2 + f_4(z, \epsilon) z^2 + f_5(z, \epsilon) z + b_2 y + f_6(y, z, \epsilon) y + f_7(\epsilon) \end{pmatrix}$$

with $f_i \in C^k$ and $f_i(0) = 0$ for all i , that is, when each of the arguments of f_i is equal to zero.

An expression for the Poincaré map Π can be derived by substituting (3.3) into the above equation. Upon making the coordinate transformation (3.5), and henceforth omitting tildes, the map Π takes the form

$$\Pi(y, z, \epsilon) = \begin{pmatrix} F_1(y, z, \epsilon) \\ F_2(y, z, \epsilon) \end{pmatrix},$$

with

$$\begin{aligned} F_1(y, z, \epsilon) &= e^\beta z + h(\epsilon) + f_1(e^\beta z + h(\epsilon), \epsilon) (e^\beta z + h(\epsilon)) + b_1 e^{\perp\alpha} (y + g(\epsilon)) \\ &\quad + f_2(e^{\perp\alpha} (y + g(\epsilon)), e^\beta z + h(\epsilon), \epsilon) e^{\perp\alpha} (y + g(\epsilon)) + f_3(\epsilon) - g(\epsilon) \\ F_2(y, z, \epsilon) &= (e^\beta z + h(\epsilon))^2 + f_4(e^\beta z + h(\epsilon), \epsilon) (e^\beta z + h(\epsilon))^2 + f_5(\epsilon) (e^\beta z + h(\epsilon)) \\ &\quad + b_2 e^{\perp\alpha} (y + g(\epsilon)) + f_6(e^{\perp\alpha} (y + g(\epsilon)), e^\beta z + h(\epsilon), \epsilon) e^{\perp\alpha} (y + g(\epsilon)) \\ &\quad + f_7(\epsilon) - e^{\perp\beta} h(\epsilon). \end{aligned}$$

For the scaling to work it is important to remove the terms of F_2 that are linear in y and to keep only terms depending on y or z in F_1 . Note that

$$\begin{aligned} f_1(e^\beta z + h(\epsilon), \epsilon) &= f_1(h(\epsilon), \epsilon) + e^\beta z \int_0^1 D_z f_1(\tau e^\beta z + h(\epsilon), \epsilon) d\tau \\ &= f_1(h(\epsilon), \epsilon) + e^\beta z D_z f_1(h(\epsilon), \epsilon) + \mathcal{O}(e^{2\beta} |z|^2). \end{aligned}$$

Then

$$\begin{aligned}
F_1(y, z, \epsilon) &= e^\beta z + h + f_1(h, \epsilon) (e^\beta z + h) \\
&\quad + b_1 e^{\perp\alpha} (y + g) + f_2(e^{\perp\alpha} g, h, \epsilon) e^{\perp\alpha} (y + g) + f_3(\epsilon) - g \\
&\quad + \mathcal{O}\left((e^{\perp\alpha} |y| + e^\beta |z|)(e^{\perp\alpha} |y + g| + |e^\beta z + h|)\right).
\end{aligned}$$

and

$$\begin{aligned}
F_2(y, z, \epsilon) &= (e^\beta z + h)^2 + f_4(h, \epsilon) (e^\beta z + h)^2 + D_z f_4(h, \epsilon) e^\beta z (e^\beta z + h)^2 \\
&\quad + f_5(\epsilon) (e^\beta z + h) + b_2 e^{\perp\alpha} (y + g) + f_6(e^{\perp\alpha} g, h, \epsilon) e^{\perp\alpha} (y + g) \\
&\quad + D_z f_6(e^{\perp\alpha} g, h, \epsilon) e^{\beta\perp\alpha} z (y + g) + f_7(\epsilon) - e^{\perp\beta} h(\epsilon) \\
&\quad + \mathcal{O}\left((e^{\perp\alpha} |y| + e^{2\beta} |z|^2)(e^{\perp\alpha} |y + g| + |e^\beta z + h|)\right).
\end{aligned}$$

In order to remove the terms of F_1 that do not depend on y and z we have to solve the equation

$$h + f_1(h, \epsilon) h + b_1 e^{\perp\alpha} g + f_2(e^{\perp\alpha} g, h, \epsilon) e^{\perp\alpha} g + f_3(\epsilon) - g = 0.$$

For the z -term of F_2 to vanish we have to satisfy the condition

$$2h + 2f_4(h, \epsilon)h + D_z f_4(h, \epsilon) h^2 + f_5(\epsilon) + D_z f_6(e^{\perp\alpha} g, h, \epsilon) e^{\perp\alpha} g = 0.$$

Obviously, $g(0) = h(0) = 0$ is a solution and by the Implicit Function Theorem the equations can be solved locally near $\epsilon = 0$. The solutions $g = g(\epsilon)$ and $h = h(\epsilon)$ determine the transformation given in Lemma 3. Note also that $h(\epsilon) = \mathcal{O}(|\epsilon|)$. Thus, the mapping Π so far has the form

$$\Pi(y, z) = \begin{pmatrix} e^\beta z + b e^{\perp\alpha} y \\ e^{2\beta} z^2 + c e^{\perp\alpha} y + \tilde{f}(\epsilon) \end{pmatrix} + \mathcal{O}\left(\begin{pmatrix} (e^\beta |z| + e^{\perp\alpha} |y|)(e^\beta |z| + e^{\perp\alpha} |y| + |\epsilon|) \\ (e^{2\beta} |z|^2 + e^{\perp\alpha} |y|)(e^\beta |z| + e^{\perp\alpha} |y| + |\epsilon|) \end{pmatrix} \right),$$

where \tilde{f} is C^k with $\tilde{f}(0) = 0$. To arrive at the form of Π given in Lemma 3 we set

$$\begin{aligned}
\tilde{\epsilon}_1 &:= \epsilon_1 \\
\tilde{\epsilon}_2 &:= \tilde{f}(\epsilon)
\end{aligned}$$

and write again ϵ_i instead of $\tilde{\epsilon}_i$. □

The following lemma completes the proof of Theorem 1.

Lemma 4 *After the scaling*

$$\begin{aligned} u &:= e^\beta y \\ v &:= e^{2\beta} z, \end{aligned}$$

the mapping Π is a diffeomorphic perturbation of the Hénon map

$$(u, v) \mapsto (v, v^2 + \delta).$$

Proof. After straightforward calculation, the scaling transformation leads to

$$\Pi(u, v, \epsilon) = \begin{pmatrix} v + b e^{\perp\alpha} u \\ v^2 + c e^{\beta\perp\alpha} u + e^{2\beta} \epsilon_2 \end{pmatrix} + \mathcal{O} \begin{pmatrix} e^{\perp\beta}(|v| + e^{\perp\alpha}|u|)(e^{\perp\beta}|v| + e^{\perp\alpha}|u| + e^\beta|\epsilon|) \\ (e^{\perp\beta}|v^2| + e^{\perp\alpha}|u|)(|v| + e^{\perp\alpha}|u| + e^\beta|\epsilon|) \end{pmatrix}.$$

To arrive at the form given in Theorem 1 set

$$(3.6) \quad \delta := e^{2\beta} \epsilon_2 = e^{\frac{2C(\epsilon)\lambda^u}{\sqrt{\epsilon_1}}} \epsilon_2.$$

Since $C(\epsilon)$ is bounded, the curves $\delta = \text{constant}$ are exponentially flat curves in (ϵ_1, ϵ_2) -space. As ϵ_1 tends to 0 (with δ fixed and therefore with $\epsilon_2 \rightarrow 0$ as well) the mapping Π tends to the mapping

$$(3.7) \quad (u, v) \mapsto (v, v^2 + \delta)$$

due to our assumption $\lambda^u < \lambda^s$.

For $\epsilon_1 > 0$, Π is clearly a diffeomorphism as it is the return map of a flow. Since we have lost one degree of differentiability in the transformation performed in Lemma 3, the map Π will be C^{k+1} . This completes the proof. \square

For the conclusions of the corollary to hold it suffices that $f \in C^3$, since our Poincaré map Π is then C^2 and a diffeomorphic perturbation of the mapping (3.7), see [PT93].

4 An example

In this section an example is constructed which exhibits the codimension-two bifurcation of the preceding theory. The general methodology of the construction is the same as in [San94b]. Numerical calculations performed on this example are then used to illustrate the results in Theorem 1 and its corollary.

4.1 Construction

The construction is carried out step by step; the final equation being given later in (4.7). We begin by considering the planar vector field

$$(4.1) \quad \begin{pmatrix} \dot{x} \\ \dot{y} \end{pmatrix} = G(y, \epsilon_1) \begin{pmatrix} -y \\ x \end{pmatrix} - \lambda^s H(x, y) \begin{pmatrix} x \\ y \end{pmatrix},$$

where $\lambda^s > 0$ and

$$(4.2) \quad \begin{aligned} G(y, \epsilon_1) &= \sin^2 \left(\frac{2\varphi + \pi}{4} \right) + \epsilon_1 = \frac{1}{2} (1 - y) + \epsilon_1 \\ H(x, y) &= \frac{1}{2} (x^2 + y^2 - 1), \end{aligned}$$

with $\varphi = \arctan \left(\frac{y}{x} \right)$. Note that (4.1) is constructed such that the zero level set of the algebraic curve $H(x, y)$, namely the unit circle

$$\Gamma = \{(x, y) / x^2 + y^2 = 1\},$$

is invariant under the flow. Note further that

$$|\nabla H(x, y)|_{\Gamma} = 1$$

and hence Γ is normally hyperbolic and attracting with exponential rate equal to $-\lambda^s$. The flow on Γ is given by

$$(4.3) \quad \dot{\varphi} = G(\varphi, \epsilon_1) = \sin^2 \left(\frac{2\varphi - \pi}{4} \right) + \epsilon_1,$$

and therefore, when $\epsilon_1 = 0$, there exists a saddle-node equilibrium p_0 at $(x, y) = (0, 1)$ with eigenvalues 0 and $-\lambda^s$. Note that the coefficient of the quadratic term in the Taylor expansion of the nonlinearity in (4.3) does not vanish. Hence, hypothesis (H4)(i) is satisfied according to the statement following (H4). With $\epsilon_1 = 0$, $\Gamma \setminus p_0$ is a homoclinic orbit to the saddle-node p_0 . Moreover, ϵ_1 unfolds the saddle-node in a generic way, in fact, $N_1 = 1$. Another way of calculating N is by computing w_c and v_c .

Upon adding a third equation via

$$(4.4) \quad \begin{pmatrix} \dot{x} \\ \dot{y} \\ \dot{z} \end{pmatrix} = \begin{pmatrix} G(y, \epsilon_1) \begin{pmatrix} -y \\ x \end{pmatrix} - \lambda^s H(x, y) \begin{pmatrix} x \\ y \end{pmatrix} \\ \lambda^u z \end{pmatrix},$$

for $\lambda^u > 0$, it is clear that (4.4) satisfies hypotheses (H1) and (H2) but that the center-stable and center-unstable manifolds intersect transversally along Γ . It remains to modify

(4.4) to ensure a quadratic tangency between $W^{cu}(p_0)$ and $W^{cs}(p_0)$. To this end, we add terms that describe a rotation along Γ which does not affect the dynamics on the invariant circle. The additional term is given by

$$(4.5) \quad \gamma H(x, y) \begin{pmatrix} 0 \\ 0 \\ 1 \end{pmatrix} - \gamma z \begin{pmatrix} H_x(x, y) \\ H_y(x, y) \\ 0 \end{pmatrix},$$

with linearization

$$\begin{pmatrix} 0 & 0 & -\gamma H_x \\ 0 & 0 & -\gamma H_y \\ \gamma H_x & \gamma H_y & 0 \end{pmatrix}$$

on Γ . With respect to the basis

$$e_1 = (0, 0, 1)^T \quad e_2 = (\nabla H, 0)^T$$

orthogonal to the tangent direction to Γ , the linearization acts according to the matrix

$$\begin{pmatrix} 0 & -\gamma \\ \gamma & 0 \end{pmatrix}.$$

We see that the rotation speed is given by γ . Multiplying (4.5) by a factor $(1 - y)$ has the effect of slowing down the rotation speed near p_0 and thus does not alter the linearization there. Arguing as in [San94b], it is not difficult to show that upon increasing γ from 0 there exists a smallest $\gamma^* > 0$ at which the degree of rotation causes a tangency to occur between $W^{cu}(p_0)$ and $W^{cs}(p_0)$.

In order to enforce this tangency to be quadratic and not of higher order we add the term

$$\begin{pmatrix} 0 \\ 0 \\ (1 - \kappa x) H^2(x, y) \end{pmatrix}$$

which again affects neither the flow nor the linearization on Γ . A proof that the tangency is quadratic for generic values of κ is postponed to an appendix.

Finally, we add the perturbation

$$-\epsilon_2 (1 - y)^2 \begin{pmatrix} 0 \\ 0 \\ 1 \end{pmatrix}$$

to break the tangency between center-stable and center-unstable manifolds. The Melnikov integral for this perturbation is given by

$$(4.6) \quad M_2 = - \int_{-\infty}^{\infty} \psi_3(t) (1 - y(t))^2 dt,$$

where ψ is the unique bounded solution of the adjoint variational equation as in (H4). Due to γ^* being defined as the first tangency for $\gamma > 0$, it can be shown as in [San94b] that $\psi_3(t)$ has a definite sign. Therefore, the integral (4.6) is clearly non-zero. Observe that $M_1 = 0$, because $\psi(t)$ is perpendicular to the tangent vector to Γ , which in turn is the derivative of the vector field with respect to ϵ_1 . Since p_0 is an equilibrium for all ϵ_2 when $\epsilon_1 = 0$, N_2 has to be zero. Thus, $M = (0, M_2)^T$ and $N = (1, 0)$ with $M_2 \neq 0$ are linearly independent and hence (H4)(ii) is satisfied.

The final example system we obtain is

$$(4.7) \quad \begin{pmatrix} \dot{x} \\ \dot{y} \\ \dot{z} \end{pmatrix} = G(y, \epsilon_1) \begin{pmatrix} -y \\ x \\ 0 \end{pmatrix} - \lambda^s H(x, y) \begin{pmatrix} x \\ y \\ 0 \end{pmatrix} + \begin{pmatrix} 0 \\ 0 \\ \lambda^u z - \epsilon_2 (1 - y)^2 \end{pmatrix} \\ + \gamma (1 - y) \begin{pmatrix} -z H_x(x, y) \\ -z H_y(x, y) \\ H(x, y) \end{pmatrix} + \begin{pmatrix} 0 \\ 0 \\ (1 - \kappa x) H^2(x, y) \end{pmatrix},$$

with G and H as in (4.2).

4.2 Numerical Results

The first step consists of determining γ^* . To this end, a defining equation is derived, solutions to which describe tangencies between the center-stable and center-unstable manifolds. This is done by using a modified adjoint variational equation

$$(4.8) \quad \dot{w} = -(A(t)^T + (\lambda^s + \eta) \text{id})w,$$

for some small $\eta > 0$, *c.f.* [San94b]. Here $A(t)$ denotes the linearization of the right hand side of (4.7) along the homoclinic solution $q(t)$ at $\epsilon = 0$. Let $\psi(t)$ be the solution of (4.8) perpendicular to $T_{q(t)}W^{cu}(p_0)$, i.e.

$$\lim_{t \rightarrow \pm\infty} \left\langle \frac{\psi(t)}{|\psi(t)|}, v_u \right\rangle = 0,$$

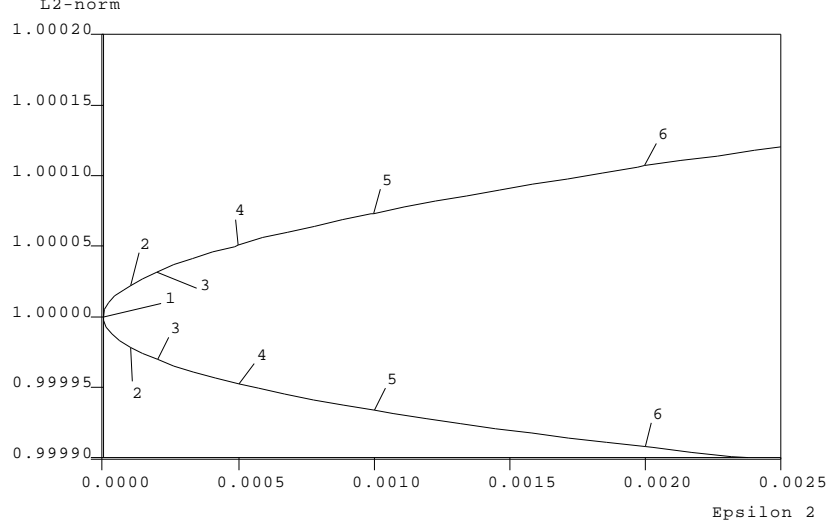


Figure 5: The L^2 -norm of the homoclinic solutions versus ϵ_2

where v_s , v_c and v_u are eigenvectors corresponding to the negative, zero and positive eigenvalues respectively. Then the additional term $(\lambda^s + \eta)\text{id}$ ensures that $\psi(t)$ converges to zero exponentially as time tends to infinity. Indeed, $\tilde{w}(t)$ solves the adjoint variational equation

$$\frac{d}{dt}\tilde{w} = -A(t)^T \tilde{w}$$

iff $w(t) = e^{\perp(\lambda^s + \eta)t} \tilde{w}(t)$ is a solution of (4.8). A tangency occurs precisely when ψ satisfies the equation

$$\lim_{t \rightarrow \infty} \left\langle \frac{\psi(t)}{|\psi(t)|}, v_s \right\rangle = 0.$$

In order to compute the homoclinic solution as well as $\psi(t)$ numerically, we have to truncate \mathbb{R} to a finite interval $[-T, T]$. Moreover, we have to add another condition which makes $\psi(t)$ unique, i.e. chooses one solution out of the family $c\psi$ for $c \in \mathbb{R}$. Using the methods in [San94b] this leads to the following system:

$$\begin{aligned} \dot{w} &= -(A(\gamma; t)^T + (\lambda^s + \eta)\text{id})w, & t \in [-T, T] \\ \langle w(-T), v_c \rangle &= 0 \\ \langle w(-T), v_u \rangle &= 0 \\ \int_{-T}^T \langle w_{old}(t), w(t) - w_{old}(t) \rangle dt &= 0, \end{aligned} \tag{4.9}$$

where $w_{old}(t)$ is a solution computed for a previous value of the continuation parameter γ . The defining equation for a tangency is given by

$$\langle w(T), v_s \rangle = 0. \tag{4.10}$$

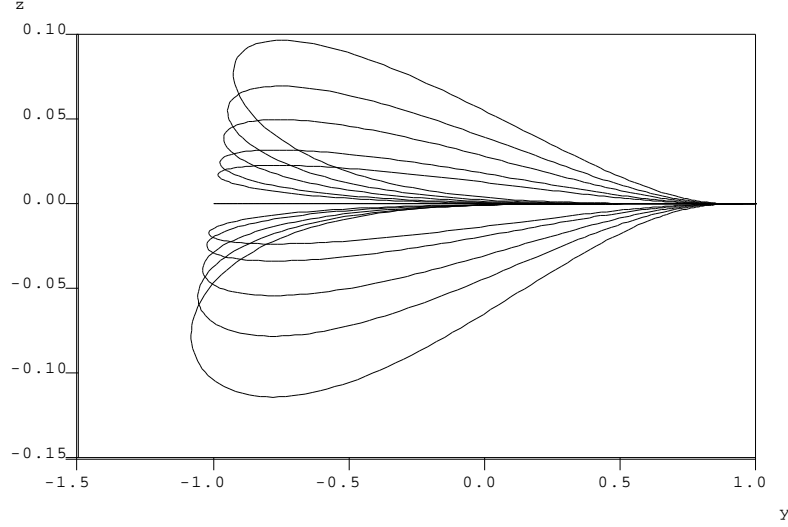


Figure 6: The (y, z) -components of the homoclinic solutions at the parameter values labelled in Figure 5

We used the code AUTO [DK86] in order to solve the system (4.9). Actually, we solved a larger system computing the saddle-node equilibrium as well as the homoclinic orbit, as in [BC94], and the solution $\psi(t)$ at the same time. This requires three parameters ϵ and γ , because we also force the circle to be invariant by introducing an additional integral condition

$$\int_{-T}^T z(t) dt = 0.$$

Using the parameter values

$$(4.11) \quad \begin{array}{ll} \lambda^s &= 2.0 & \kappa &= 0.0 \\ \lambda^u &= 1.0 & T &= 1000.0, \end{array}$$

we computed γ^* to be

$$(4.12) \quad \gamma^* = 0.9220712$$

for $(\epsilon_1, \epsilon_2) = 0$.

Remark 1 *The method used for the detection of the tangency was specific to our constructed example. In practise, a tangency would be detected by following a path of homoclinic solutions and encountering a limit point rather than solving the adjoint variational equation.*

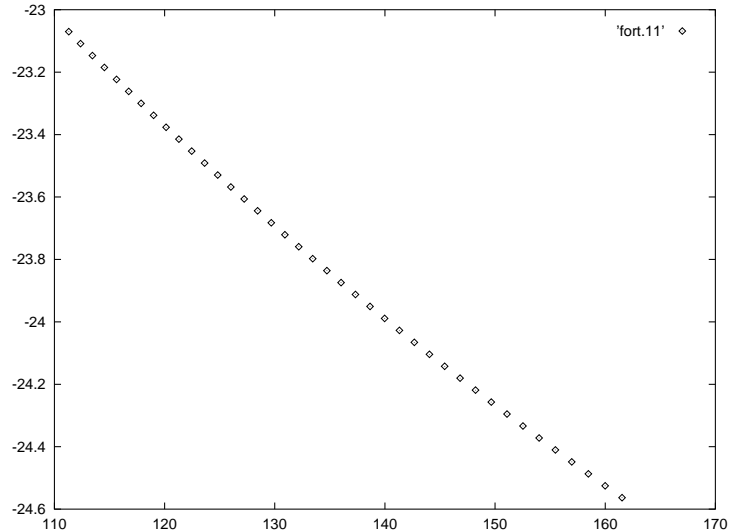


Figure 7: The period-doubling curve (plotted as $\log(\epsilon_2)$ versus $1/\sqrt{\epsilon_1}$)

Figures 5 and 6 show numerical results of the computation of the saddle-node of homoclinic solutions merging at $\epsilon = 0$ for the parameter values given in (4.11) and (4.12). Figure 7 illustrates the asymptotic scaling behaviour of system (4.7). The primary period-doubling curve appearing in the Hénon map is computed and plotted in a logarithmic scale corresponding to the scaling (3.6) used in the proof.

5 Discussion

One motivation for this work was to describe a natural two-parameter situation which contains the codimension-one mechanism for chaos described by Shilnikov [Shi69], caused by the existence of more than one homoclinic orbit to a saddle-node. In contrast to his by now famous work on another codimension-one mechanism, namely that caused by a homoclinic orbit to a saddle-focus equilibrium [Shi70], the former has received little or no attention in applications. In fact, we are unaware of any previous example in the literature which exhibits this bifurcation (see the open problem in [Gle88, p. 145]). We hope that this paper, together with numerical methods for the continuation of saddle-node homoclinic orbits, in [BC94] for example, will provide the applied scientist with an appropriate tool kit for finding and analyzing the consequences of this mechanism in specific examples. Upon two-parameter continuation along a branch of saddle-node homoclinics, one need only detect a limit point with respect to a parameter, and generically the bifurcation sequences

described by Theorem 1 and its corollary must occur.

As we have shown in Theorem 1, the unfolding of a quadratic tangency of the center-unstable and center-stable manifolds of a saddle-node equilibrium contains the Hénon map. Actually, another motivation for our work was the article by Homburg, Kokubu and Krupa [HKK93]. They conjectured that similar behaviour should occur near an inclination-flip bifurcation due to the annihilation of a horseshoe. Up to now their conjecture remains unsolved. In contrast to the results expected for flip bifurcations, the horseshoe exists in a large region of parameter space in the case studied here. Indeed, it is almost one quadrant in \mathbb{R}^2 . Another contrast with the flip-bifurcations is that here the scaling of parameters depends only on the eigenvalue closest to zero rather than on the ratio of stable and unstable eigenvalues as expected for flip bifurcations. The reason is that the “time of flight” does not depend on the non-zero eigenvalues.

Fiedler [Fie92] has already proved that a non-transverse homoclinic orbit to a saddle-node cannot be stratified (in his terminology) and thus must be accompanied by complicated behaviour, for topological reasons. Indeed, as he pointed out, a certain topological index of one of the homoclinic orbits existing for $\epsilon_2 > 0$ must be ± 1 , while the index of the other is 0. Hence it is not possible to continue the index continuously through the bifurcation point. However, there do not exist any N -homoclinic solutions in the unfolding of the codimension-two point. In fact, if one considers only homoclinic and heteroclinic orbits, the bifurcation is quite simple; only the two homoclinic solutions and the heteroclinic loop described in Theorem 1 exist in a neighborhood of the bifurcation, see Figure 4. Hence the topological index introduced by Fiedler [Fie92] appears to be strongly affected by the nearby dynamics stemming from the periodic and aperiodic solutions.

The results in [Shi69] also apply in higher dimensions, including the case where some or all of the non-zero eigenvalues of the saddle-node are complex. The existence of a quadratic tangency in the complex case must therefore also force the creation of shift dynamics. Though our analysis relied on the fact that the hyperbolic eigenvalues were real, the methods used should be readily applicable to cases where complex eigenvalues are present. In particular, the Poincaré map can be constructed in a similar manner. The resulting map, however, would be defined on a higher dimensional section and no description in terms of a well-known mapping like the Hénon map seems available. Hence the precise annihilation mechanism of the horseshoe in this case remains unknown.

In addition to the two homoclinic solutions disappearing in a limit point bifurcation, other

- say k - homoclinic orbits may exist as transverse intersections of the center-stable and center-unstable manifolds for the same parameter value. Then, as well as the creation of a shift on two symbols due to the saddle-node of the homoclinic orbits, a shift on $k + 2$ symbols must be created from a shift on k symbols, by Shilnikov's results. It should be possible to use the analysis presented here in order to investigate this scenario also.

In the introduction, another bifurcation was mentioned involving a homoclinic orbit to a saddle-node equilibrium. There, the homoclinic solution is contained in the intersection of stable and center-unstable manifolds, for example. Assuming that k additional homoclinic solutions are present as transverse intersections of center-stable and center-unstable manifolds, again a shift on $k + 1$ symbols bifurcates from a shift on k symbols. The mechanism is likely to be described by a Hénon-like map, although we are not aware of rigorous results.

Appendix A. The quadratic tangency

We start by rewriting (4.7) in the form

$$(A.1) \quad \begin{pmatrix} \dot{x} \\ \dot{y} \\ \dot{z} \end{pmatrix} = f(x, y, z) + \begin{pmatrix} 0 \\ 0 \\ (1 - \kappa x) H^2(x, y) \end{pmatrix} =: F(x, y, z).$$

Throughout this section, ϵ is equal to zero. Moreover, we shift time such that $q(0) = (0, -1, 0)$. The aim of the appendix is to prove that the second term in (A.1) ensures a quadratic tangency of $W^{cu}(p_0)$ and $W^{cs}(p_0)$ for generic values of κ . The first step is to derive an expression for the quadratic terms of the expansion of the center-stable manifold at $q(0)$. To this end, define

$$\Sigma^i := q(0) + \eta_1 v_i(0) + \eta_2 \psi(0), \quad i = s, u,$$

for small $\eta \in \mathbb{R}^2$, as sections transverse to the homoclinic orbit at $q(0)$. Here $v_i(0) \in T_{q(0)}\mathcal{F}^i$ denotes a unit vector in the tangent space of the stable (unstable) fibre \mathcal{F}^i of the center-stable (center-unstable) manifold for $i = s$ ($i = u$). Furthermore, $\psi(t)$ is the unique bounded solution of the adjoint variational equation mentioned in section 2. We will compute the coefficients of the quadratic terms describing the intersection of the center-stable and center-unstable manifolds with Σ^s or Σ^u respectively as graphs over the common tangent space $T_{q(0)}W^{cs}(p_0) = T_{q(0)}W^{cu}(p_0)$. However, an easy calculation, using the fact

that the homoclinic orbit is contained in $W^{cu}(p_0)$ and $W^{cs}(p_0)$, shows that these coefficients do not depend on this specific choice of sections.

Now, let $u(t)$ be a solution of (A.1) lying in the center-stable manifold close to $q(t)$ such that $u(0) \in \Sigma^s$. Decompose this solution as

$$u(t) = q(t) + y(t),$$

where $y(t)$ satisfies

$$\dot{y}(t) = DF(q(t))y + (F(q(t) + y(t)) - F(q(t)) - DF(q(t))y).$$

Since we are interested in second-order terms, $y(t)$ can be decomposed into

$$y(t) = \nu v_s(t) + \nu^2 z(t),$$

for ν small, where $v_s(t) \in T_{q(t)}\mathcal{F}^s$ was defined above. Note that $v_s(t)$ converges exponentially to zero as time tends to infinity due to $v_s(0) \in T_{q(0)}\mathcal{F}^s$. A straightforward calculation shows that z satisfies

$$\begin{aligned} \dot{z} &= DF(q)z + \frac{1}{2}D^2F(q)[v_s, v_s] + \mathcal{O}(\nu(|z| + |v_s|^2)(\nu|z| + |v_s|)) \\ &= DF(q)z + \frac{1}{2}D^2F(q)[v_s, v_s] + \mathcal{O}(\nu). \end{aligned}$$

The coefficient of the quadratic term in the expansion of $W^{cs}(p_0) \cap \Sigma^s$ is therefore equal to $w_s(0)$, where $w_s(t)$ denotes the unique bounded solution of

$$\dot{w} = DF(q)w + \frac{1}{2}D^2F(q)[v_s, v_s]$$

satisfying $\langle w(0), v_s(0) \rangle = 0$. Moreover, $w_s(0)$ is given by

$$w_s(0) = \int_{-\infty}^0 \langle \psi(t), D^2F(q(t))[v_s(t), v_s(t)] \rangle dt.$$

Proceeding in the same manner for the quadratic term of the center-unstable manifold we obtain finally the quadratic coefficients

$$\begin{aligned} (A.2) \quad c_s &:= w_s(0) = \int_{-\infty}^0 \langle \psi(t), D^2F(q(t))[v_s(t), v_s(t)] \rangle dt \\ c_u &:= w_u(0) = \int_{-\infty}^0 \langle \psi(t), D^2F(q(t))[v_u(t), v_u(t)] \rangle dt. \end{aligned}$$

Next, we compute the coefficients by substituting the vector field (A.1) into (A.2). The third component of the second derivative of $(0, 0, (1 - \kappa x)H^2(x, y))^T$ is given by the matrix

$$2(1 - \kappa x) \begin{pmatrix} x^2 & xy & 0 \\ xy & y^2 & 0 \\ 0 & 0 & 0 \end{pmatrix}.$$

Decomposing

$$v_i(t) = \alpha_i(t) \begin{pmatrix} -y(t) \\ x(t) \\ 0 \end{pmatrix} + \beta_i(t) \begin{pmatrix} x(t) \\ y(t) \\ 0 \end{pmatrix} + \gamma_i(t) \begin{pmatrix} 0 \\ 0 \\ 1 \end{pmatrix}$$

for $i = s, u$ yields

$$D^2\left((1 - \kappa x) H^2(x, y)\right)[v_i, v_i] = 2(1 - \kappa x) \beta_i^2.$$

Hence we obtain for (A.2)

$$\begin{aligned} c_s(\kappa) &= \int_{-\infty}^0 (\langle \psi(t), D^2 f(q(t), 0)[v_s(t), v_s(t)] \rangle + 2\psi_3(t)(1 - \kappa x(t))\beta_s(t)^2) dt \\ c_u(\kappa) &= \int_{-\infty}^0 (\langle \psi(t), D^2 f(q(t), 0)[v_u(t), v_u(t)] \rangle + 2\psi_3(t)(1 - \kappa x(t))\beta_u(t)^2) dt, \end{aligned}$$

where $q(t)$ is denoted by $(x(t), y(t), 0)$. Suppose that $c_s(0) = c_u(0)$. The derivative of the coefficients with respect to κ are given by

$$\begin{aligned} D_\kappa c_s(0) &= -2 \int_{-\infty}^0 \psi_3(t) x(t) \beta_s(t)^2 dt \\ D_\kappa c_u(0) &= -2 \int_{-\infty}^0 \psi_3(t) x(t) \beta_u(t)^2 dt. \end{aligned}$$

Recall that $\psi_3(t)$ possesses a definite sign. Moreover, $\beta_s(t)$ is non-zero for large times. Therefore, at least $D_\kappa c_s(0)$ is non-zero. Furthermore, note that $D_\kappa c_s(0)$ and $D_\kappa c_u(0)$ are of different sign because $x(t)$ is positive or negative for t positive or negative, respectively. This proves that $c_s(\kappa)$ and $c_u(\kappa)$ do not coincide as soon as κ becomes non-zero and hence the existence of a quadratic tangency of the example is proved for generic values of κ .

References

- [BC94] F. Bai and A.R. Champneys. *Numerical detection and continuation of saddle-node homoclinic bifurcations of codimension one or two*. Preprint, University of Bath, 1994.
- [CK94] A. Champneys and Yu. A. Kuznetsov. *Numerical detection and continuation of codimension-two homoclinic bifurcations*. Int. J. Bifurcation & Chaos, **4** (1994), 785–822.
- [CL90] S.-N. Chow and X. B. Lin. *Bifurcation of a homoclinic orbit with a saddle-node equilibrium*. Diff. Integr. Eq., **3** (1990), 435–466.

- [Den90] B. Deng. *Homoclinic bifurcations with nonhyperbolic equilibria*. SIAM J. Math. Anal., **21** (1990), 693–720.
- [DK86] E. Doedel and J. Kernévez. *AUTO: Software for continuation problems in ordinary differential equations with applications*. Technical report, California Institute of Technology, 1986.
- [Fie92] B. Fiedler. *Global pathfollowing of homoclinic orbits in two-parameter flows*. Preprint, 1992.
- [GH90] J. Guckenheimer and P. Holmes. *Nonlinear Oscillations, Dynamical Systems and Bifurcations of Vector Fields*. Springer-Verlag, New York, 1990.
- [Gle88] P. Glendinning. *Global bifurcation in flows*. In *New directions in dynamical systems* (T. Bedford and J. Swift, editors), pages 120–149. Cambridge University Press, 1988.
- [HKK93] A. J. Homburg, H. Kokubu, and M. Krupa. *The cusp horseshoe and its bifurcations from inclination-flip homoclinic orbits*. Preprint, 1993.
- [IY91] Yu. S. Il'yanshenko and S. Yu. Yakovenko. *Finitely-smooth normal forms of local families of diffeomorphisms and vector fields*. Russian Math. Surveys, **46** (1991), 1–43.
- [Luk82] V.I. Lukyanov. *Bifurcations of dynamical systems with a saddle-node separatrix loop*. Diff. Eq., **18** (1982), 1049–1059.
- [MV93] L. Mora and M. Viana. *Abundance of strange attractors*. Acta. Math., **171** (1993), 1–71.
- [PT93] J. Palis and F. Takens. *Hyperbolicity and sensitive chaotic dynamics at homoclinic bifurcations*. Cambridge University Press, 1993.
- [San93] B. Sandstede. *Verzweigungstheorie homokliner Verdopplungen*. Doctoral thesis, University of Stuttgart, 1993.
- [San94a] B. Sandstede. *Center manifolds for homoclinic solutions*. In preparation, 1994.
- [San94b] B. Sandstede. *Constructing dynamical systems possessing homoclinic bifurcation points of codimension two*. In preparation, 1994.

- [Sch87] S. Schecter. *The saddle-node separatrix-loop bifurcation*. SIAM J. Math. Anal., **28** (1987), 1142–1156.
- [Shi69] L.P. Shilnikov. *On a new type of bifurcation of multidimensional dynamical systems*. Soviet Math. Dokl., **10** (1969), 1368–1371.
- [Shi70] L.P. Shilnikov. *A contribution to a problem of the structure of an extended neighborhood of a rough equilibrium state of saddle-focus type*. Math. USSR Sbornik, **10** (1970), 91–102.
- [Sot74] J. Sotomayor. *Generic one-parameter families of vector fields*. Inst. Hautes Etudes Sci. Publ. Math., **43** (1974), 5–46.
- [Van89] A. Vanderbauwhede. *Centre manifolds, normal forms and elementary bifurcations*. In *Dynamics reported* (U. Kirchgraber and H.O. Walther, editors), volume 2, pages 89–169. Wiley and Sons, 1989.
- [YA85] J. A. Yorke and K. T. Alligood. *Period doubling cascades of attractors: a prerequisite for horseshoes*. Comm. Math. Phys., **101** (1985), 305–321.